Intrinsic thermo-acoustic instability criteria based on frequency response of flame transfer function

Intrinsic thermo-acoustic instability criteria based on frequency response of flame transfer function

Mohammad Kojourimanesh[1], Viktor Kornilov[2], Philip de Goey[3]
Eindhoven University of Technology
Dept. of Mechanical Engineering, TU/e, Eindhoven, The Netherlands

Ines Lopez Arteaga[4]
Eindhoven University of Technology & KTH Royal Institute of Technology
Dept. of Mechanical Engineering, TU/e, Eindhoven, The Netherlands
Dept. of Engineering Mechanics, KTH, Stockholm, Sweden

ABSTRACT

A study of Intrinsic Thermo-Acoustic (ITA) instability behavior of flames anchored to a burner deck is performed by introducing a mapping between the Flame Transfer Function, FTF(s), defined in the complex (Laplace) domain and the experimentally measured Flame Frequency Response, FFR(iω). The conventional approach requires a system identification procedure to obtain the FTF(s) from the measured FFR(iω). Next, root-finding techniques are applied to define the complex eigenfrequencies. The common practice is to fit the FTF(s) by a rational function that may lead to artifacts like spurious poles and zeros. The purpose of the present work is to establish instability criteria which are directly applicable in the frequency domain. The particular case is considered where the acoustic boundary conditions at both sides of the flame are anechoic. Therefore, the pure ITA mode is treated. First, the causality of the measured FFR(iω) is checked. Then, the criteria of the ITA mode instability applicable to the FFR(iω) phase and magnitude, are derived. Causality properties are used to find the unstable frequency, growth rate, and even the maximum possible value of the linear growth rate. In addition, a procedure is explained to reconstruct the flame transfer function in the complex plane ***s*** *from the measured flame frequency response which could be an alternative method to study the FTF behavior in the complex domain instead of its estimation with a rational function.*

1. INTRODUCTION

Modeling the (in-)stability of thermo-acoustic systems within the network modeling approach requires an analysis in the complex (Laplace) domain. This means that for all elements of the model, including a burner with flame, the descriptions should be obtained in terms of functions of complex frequency ($s = \sigma + i\omega$). However, with current technologies, it is only possible to measure the Flame Frequency Response ($FFR_{i\omega}$) as a function of linear/circular frequency ω. Therefore, a system identification procedure is required to obtain the Flame Transfer Function in the complex plane, FTF_s. Several studies have been conducted to model FTF_s from the measured $FFR_{i\omega}$ [1,2]. In addition, a few studies, such as in [3], have tried to find a relationship between the flame transfer function in the

[1] m.kojourimanesh@tue.nl
[2] v.kornilov@tue.nl
[3] L.P.H.d.Goey@tue.nl
[4] i.lopez@tue.nl

complex domain and the flame frequency response. Attempts to develop alternative approaches when the instability criteria are directly based on the analysis of the flame frequency response are still limited. For example, the *Nyquist criterion* is based on the *Argument principal* and is a well-known technique in *Control Theory* that is also commonly used in the analysis of thermo-acoustic systems. The Nyquist plot (the polar plot of the frequency response) is used to find the differences of the number of poles and zeros of the system in the right half plane (RHP) of the complex domain. This technique makes it possible to resolve the dilemma of (in-)stability of the system. However, this approach does not provide direct information about the unstable frequencies and growth rates. In a pioneer work Kopitz and Polifke proposed an approach how to estimate the unstable frequency and growth rate directly from the polar plot of the Open-Loop system Transfer Function (OLTF) without solving the dispersion relation [4]. The goal of this work is to further extend this methodology to provide insight into system design techniques to ensure the operational stability of an appliance.

2. FORMULATION

There is a large group of burners in which the heat release rate is particularly and exclusively sensitive to velocity perturbations on the upstream side of the flame. Thermo-acoustic characteristics of these compact velocity-sensitive flames can be described with the definition of their FTF_s. In literature like [4–6], it has been shown that the Flame Transfer Matrix (FTM), which describes the linear relationship between the acoustic pressure and velocity fluctuations at the upstream of the burner/flame (p'_{up}, u'_{up}) and at the downstream of it (p'_{dn}, u'_{dn}) is linearly related to the burner with flame transfer function and in the limit of zero mean flow Mach number the link is the following:

$$\begin{Bmatrix} p'_{dn} \\ u'_{dn} \end{Bmatrix} = \begin{bmatrix} 1 & 0 \\ 0 & 1+\theta\, FTF_s \end{bmatrix} \begin{Bmatrix} p'_{up} \\ u'_{up} \end{Bmatrix}, \tag{1}$$

where $\theta = (\overline{T_{dn}}/\overline{T_{up}}) - 1$ is the temperature ratio; $\overline{T_{up}}, \overline{T_{dn}}$ being the mean temperature at the upstream and downstream sides of the flame. In terms of Riemann invariants (f, g), defined as $f \stackrel{\text{def}}{=} \frac{1}{2}\left(\frac{p}{\rho_0 c} + u\right)$, $g \stackrel{\text{def}}{=} \frac{1}{2}\left(\frac{p}{\rho_0 c} - u\right)$ and shown in Figure 1, the fluctuations of pressure and velocity can be written as

$$\begin{cases} (f_2 + g_2) = \varepsilon(f_1 + g_1) \\ f_2 - g_2 = (1 + \theta\, FTF_s)\,(f_1 - g_1) \end{cases}, \tag{2}$$

where $\varepsilon = \frac{\rho_{up} c_{up}}{\rho_{dn} c_{dn}}$ is the jump in characteristic acoustic impedance across the flame.

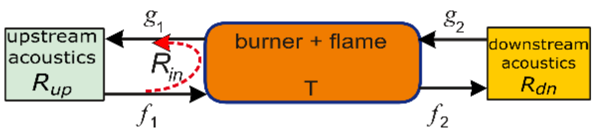

Figure 1: Generic representation of thermo-acoustic of a combustion system.

2.1. Thermo-acoustic system matrix

Riemann invariants at the upstream and downstream sides of the flame are related with the reflection coefficients at both sides, i.e., $R_{\text{up}} = f_1/g_1$, $R_{\text{dn}} = g_2/f_2$. Therefore, by substituting f_1 and g_2 in Equation 2, one can derive the full system matrix expression of a thermo-acoustic system as follows:

$$\begin{bmatrix} (1 + R_{\text{up}})\varepsilon & -(1 + R_{\text{dn}}) \\ (1 + \theta\, FTF_s)(R_{\text{up}} - 1) & (R_{\text{dn}} - 1) \end{bmatrix} \begin{Bmatrix} g_1 \\ f_2 \end{Bmatrix} = \begin{Bmatrix} 0 \\ 0 \end{Bmatrix}. \tag{3}$$

For $1+\theta\, FTF_s \neq 0$, the eigenvalues of the system will be obtained from the dispersion relation, i.e., the requirement that the determinant of the thermo-acoustic system matrix equals zero. The dispersion relation of the thermo-acoustic system is given by

$$\Psi\, \varepsilon + 1 + \theta\, FTF_{s_0} = 0, \tag{4}$$

where $\Psi = \frac{(1+R_{up})}{(1-R_{up})}\frac{(1-R_{dn})}{(1+R_{dn})}$ is a function which incorporates information about acoustics of the terminations with respect to the burner element. For the case of $1+\theta\, FTF_s = 0$, Equation 4 cannot be used, and one can use only $\frac{1}{\theta} + FTF_s = 0$.

2.2. Intrinsic Thermo-Acoustic (ITA) instability equation

To elucidate features of purely intrinsic thermo-acoustic system modes, one should apply anechoic terminations at both sides of the flame in Equations 3 and 4, i.e., $R_{\mathrm{up}} = 0, R_{\mathrm{dn}} = 0$. Therefore, $\Psi = 1$ and Equation 4 reduces to so called the "intrinsic instability equation" [4,7]

$$n_0 + FTF_{s_0} = 0, \tag{5}$$

where n_0 is a real positive number which depends on ε and θ as $n_0 = \left|\frac{\varepsilon+1}{\theta}\right|$. By applying the two equations $c^2 = \gamma RT$ and $P = \rho RT$ for the perfect (ideal) gas with considering constant pressure before and after the compact thin flame, one can derive the value of n_0 as $n_0 \cong \sqrt{\frac{\bar{T}_{dn}}{\bar{T}_{up}}} + 1 \Big/ \frac{\bar{T}_{dn}}{\bar{T}_{up}} - 1$. The case ${}^{1}\!/_{\theta} + FTF_s = 0$ is similar to the intrinsic mode and it can be treated with the same strategy expressed below. If the flame transfer function in the complex domain, FTF_s, is known, then the roots of Equation 5, s_0, are found when the $\left|FTF_{s_0}\right| = n_0$ and $\angle FTF_{s_0} = \pi, 3\pi, \ldots$ which needs to be searched in the complex plane. In most cases, flame transfer functions are complicated functions, therefore the roots cannot be found analytically, except for the case of simple models. In most cases, the analytical form of the flame transfer function in the complex domain is unknown, as only the flame frequency response ($FFR_{i\omega}$) can be measured. Therefore, to determine the intrinsic mode of the system, two approaches can be considered. The first one consists of modeling the flame transfer function in Laplace domain guessing a form of its functional dependence and then solving Equation 5 as in [6]. The second approach includes finding special criteria of presents of unstable roots based directly on the analysis of the measured flame frequency response in the frequency domain as in [4]. This approach supposes using certain properties of causal functions.

2.3. Causal function properties and Causality check

It is known that the functions which describe input-to-output relations of physical systems should satisfy the requirement that they are causal in the sense that the future of the input signal cannot influence the past of the output signal. In stable physical systems, causality implies the condition of analyticity in the Right Half Plane (RHP) of the complex domain ($s - plane$) and, conversely, analyticity in the RHP implies causality of the corresponding stable physical system [8]. An "analytic" function in the RHP implies that there is no pole in the RHP. Any mapping by an analytic function is *conformal*, i.e., it preserves local angles, at any point when it has a non-zero derivative [4].

In case of applying the advances of causal systems to measured data, such as the measured flame frequency response $FFR_{i\omega}$, one could first check the causality of the measured data. To do this, one can calculate the real part of a causal function from the imaginary part of the measured data using the Kramers-Kronig relations [9] and then compare the measured real part with the derived real part of this causal function and do the reverse for the imaginary part. The next option is to apply the Hilbert transform property to determine the causality of the system, as in [10]. However, a better method was developed by Barannyk et al. [11] as an SVD-based Fourier continuations algorithm to fit a Fourier series with a finite number (M) of periodic and causal functions to the measured data. The goal is to construct an accurate Fourier series approximation of $FFR_{i\omega}$ in a given frequency domain which is

$$\mathrm{C}(FFR)(x_j) = \sum_{k=1}^{M} \alpha_k \, e^{-\frac{2\pi i}{b} k \, x_j} \, , \tag{6}$$

where $x_j = \frac{0.5}{\omega_{max}} \omega_j$ is the normalized discrete frequency in the frequency range of $[0, \omega_{max}]$, b is the period of the approximation, usually chosen as the length of the domain times two or four, and α_k coefficients which are generated by applying the truncated SVD method [11]. The order of the error between the measured data and the causal function would be a good indication for checking the causality of the given data. It is obvious that the error estimates should decrease as the number M increases. The method is accurate, reliable, and capable of detecting very small-localized causality violations with amplitudes close to machine precision. It has been successfully tested on several analytical functions and measured flame frequency responses. For instance, for a perforated burner deck with hole diameter of 2 mm and a pitch of 4.5 mm (D2P4.5), at $\varphi = 0.8, \mathrm{V} = 80 \text{ cm/s}$, the error between the measured FFR and the closest causal function derived from a Fourier series of M periodic causal functions (varying from 100 to 500) is shown in Figure 2.

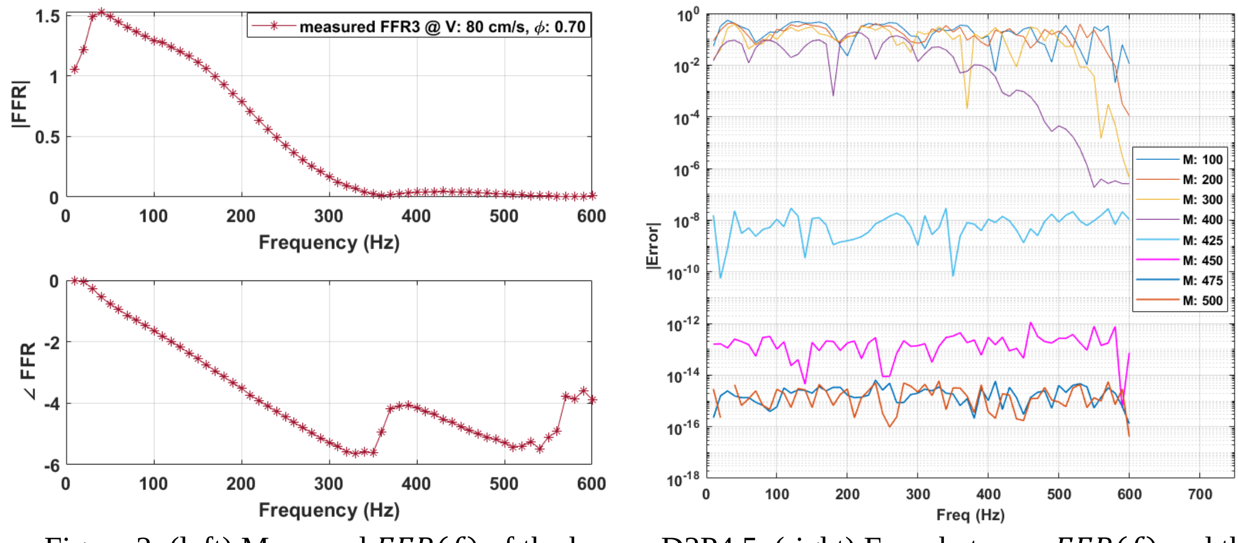

Figure 2: (left) Measured $FFR(f)$ of the burner D2P4.5, (right) Error between $FFR(f)$ and the closest causal function derived from a Fourier series of M periodic causal functions.

2.4. Stability and instability criteria of ITA mode

For a measured FFR, the number of unstable system modes of the intrinsic thermo-acoustic nature is equal to the number of times $FFR_{i\omega}$ encircles the point $(-n_0, 0)$ clockwise. Consequently, for the system to be intrinsically stable it is sufficient if for $FFR_{i\omega}$, in the frequency range of $0 < \omega < +\infty$ one of the following conditions is satisfied

- the phase of $FFR_{i\omega}$ does not cross $-\pi$, i.e., $-\pi < \angle FFR_{i\omega} < 0$, or
- when the phase of $FFR_{i\omega}$ crosses $-\pi$, the real part of $FFR_{i\omega}$ is less than n_0, i.e., $|\Re(FFR_{i\omega \to -\pi})| < n_0$.

Proof. Based on the Argument principal, if the polar plot of a function does not turn around the critical point, $(-n_0, 0)$, then it signifies that the number of poles N_p and zeros N_z in the RHP is equal (or $N_p > N_z$). If the causality check shows that $FFR_{i\omega}$ is an analytic function in the RHP, then it means that there is no RHP pole, therefore, $N_z = 0$ means that the system is stable.

2.5. The unstable intrinsic frequency, the growth rate and the bounds

For causal systems, Kopitz and Polifke have shown in [4] that the frequency of an unstable mode (ω_0) is approximately equal to the frequency where the distance between the critical point $(-1 + i0)$ and the polar plot of the OLTF reaches a local minimum. The growth/decay rate is approximately equal to the minimum distance between the critical point and the OLTF image curve divided by the mapping scale factor. "*The scaling factor can be determined by evaluating how an interval* $(\omega_0 - \Delta\omega \to \omega_0 + \Delta\omega)$*, is mapped to a segment* $TF(\omega_0 - \Delta\omega) \to TF(\omega_0 + \Delta\omega)$ *of the OLTF image curve. The scaling factor is then estimated as the arc length divided by* $2\Delta\omega$ *in the limit* $\Delta\omega \to 0$" [4]. However, it would be more accurate to consider the scaling factor as the linear distance (not the arc length) between the points before and after the unstable frequency, since the linear distance (not the arc length) between the critical point and the OLTF plot is used: $\frac{\sigma_0}{2\Delta\omega} = \frac{Arc(TF(\omega_0) - \text{point}(-1))}{Arc(TF(\omega_2) - TF(\omega_1))} = \frac{|TF(\omega_0) - \text{point}(-1)|}{|TF(\omega_2) - TF(\omega_1)|}$.

Therefore, for the intrinsic instability, the assessment of the polar plot of the measured $FFR(f)$ can be used to determine the (in)stability, the frequency of unstable oscillation, and the oscillation linear growth rate.

If the polar plot of the measured FFR_f turns around the point $(-n_0 + i0)$, then the system is unstable. A good approximation of the unstable frequency would be the frequency in the Lefthand side of this point at the FFR_f polar plot, i.e., $|\Re(FFR_f)| > n_0$, which has a minimum distance from this point. The distance divided by the scaling factor gives the positive growth rate, i.e.,

$$\sigma_0 = \frac{2\Delta\omega \, |FFR_{i\omega_0} - n_0|}{|FFR_{i(\omega_0 + \Delta\omega)} - FFR_{i(\omega_0 - \Delta\omega)}|} \,. \tag{7}$$

The maximum possible growth rate of the intrinsic thermo-acoustic system can be reached if the maximum value of the FFR_f occurs in the $-\pi$ phase. Then, the maximum growth rate would be

$$\sigma_{max} = \frac{2\Delta\omega \, |Max(FFR_{i\omega_{-\pi}}) - n_0|}{|FFR_{i(\omega_{-\pi} + \Delta\omega)} - FFR_{i(\omega_{-\pi} - \Delta\omega)}|} \,. \tag{8}$$

Also, the minimum possible positive growth rate of the intrinsic thermo-acoustic system can happen if the maximum value of the FFR_f occurs at frequency where $|\Re(FFR_f)| = n_0$.

Proof. From Equation 7, it is evident that for the $\sigma_{min} = 0$ it is needed to $FFR_{i\omega_0} = n_0$, and to obtain σ_{max}, $FFR_{i\omega_0}$should be equal to $Max(FFR_{i\omega})$. Therefore, $FTF_{s=\sigma_0+i\omega_0}$ should also be the maximum of $Max(FTF_{s=\sigma_0+i\omega})$ due to conformality. The local maximum of line $FTF_{s=\sigma_0+i\omega}$ at $s_0 = \sigma_0 + i\,\omega_0$ means that the polar plot of FTF_s is normal to the real axis, i.e., $\angle FTF_{s=\sigma_0+i\omega_0} = \pi/2$ and the conformality says this should also be the case in the frequency response, i.e., $\angle FFR_{i\omega_0 = i\omega_{-\pi}} = \pi/2$.

To show the above statement in terms of a graphical fashion, three FFR_f of the perforated burner D2P4.5 at three conditions of the equivalence ratio and the velocity are measured. The polar plots of them are shown in Figure 3. A pink color indicates the area where the unstable frequency (ω_0) must be found for any of them.

The maximum value of $|FFR_f|$ for these flame frequency responses are 1.03,1.17, and 1.53 respectively. The maximum value of $FFR3$ is higher than $FFR2$, however, as can be seen in Figure 3, the angle $\angle FFR2$ is higher than $\angle FFR3$ at the unstable frequency ($s_0 = \sigma_0 + i\omega_0$) which is more important. Therefore, the value of the growth rate for the $FFR2$ is bigger than one for $FFR3$.
Moreover, the $\angle FFR2 \approx \pi/2$ therefore, the case of maximum possible linear grow rate of ITA mode is realized for this combustion conditions for the same maximum value of $|\Re(FFR)|$.

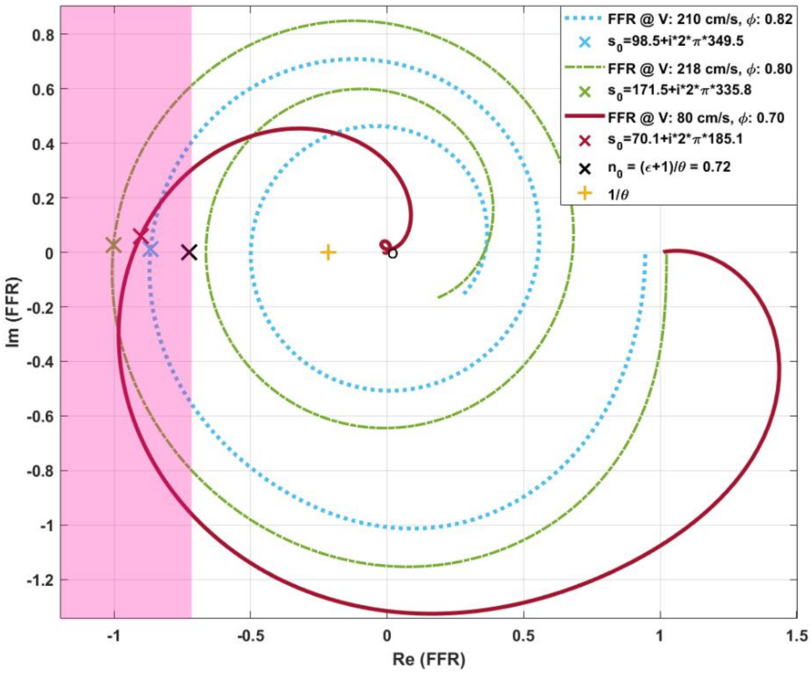

Figure 3: Three Measured $FFR(f)$ of the burner D2P4.5 and the unstable frequency region.

2.6. FTF reconstruction in the complex domain

An alternative approach to extend the measured frequency response to the FTF plane by fitting it with a rational function can be considered. If the measured FFR is causal, then it is possible to reconstruct the FTF at least for $\sigma > 0$ from the measured $FFR_{i\omega}$using the conformal mapping property of causal functions. The procedure could be as follows.
1) Find the location of the unstable frequency ω_0 in the polar plot of $FFR_{i\omega}$.
2) Measure the angle of $FFR_{i\omega_0}$and because of the conformality (between Figure 4a and Figure 4b) represent this angle as the angle of $FTF_{s_0=\sigma_0+i\omega_0}$at the point $(-n_0 + i0)$, i.e., $\angle FTF_{s=\sigma_0+i\omega_\text{j}} = \alpha$. Therefore, the first point (j) of FTF is reconstructed at the critical point with slope angle of α which is needed for finding the neighbor points.
3) Calculate the growth rate from Equation 7.
4) For each point $(j+1)$ after the critical point on the line $s = \sigma_0 + i\omega$, calculate the scaling factor based on $r_{j+1} = \sigma_0 \frac{\left|FFR_{i(\omega_{j+1})} - FFR_{i(\omega_j)}\right|}{\Delta\omega}$ and then plot a circle with this radius and center of $FFR_{i(\omega_{j+1})}$.
5) Find a point on this circle that has the same angle as $\angle FFR_{s=i\omega_\text{j}}$. That point would be the next reconstructed point (j+1) of FTF on the line $s = \sigma_0 + i\omega$.
6) Repeat this procedure for all points after and before the critical point on the line $s = \sigma_0 + i\omega$ as shown in Figure 4c.

7) Subsequently, this procedure can be repeated for other fixed values of σ, to reconstruct the polar plot of the line $FTF_{s=\sigma+i\omega}$. The results for $\sigma > 0$ could be plotted similar to Figure 4d.

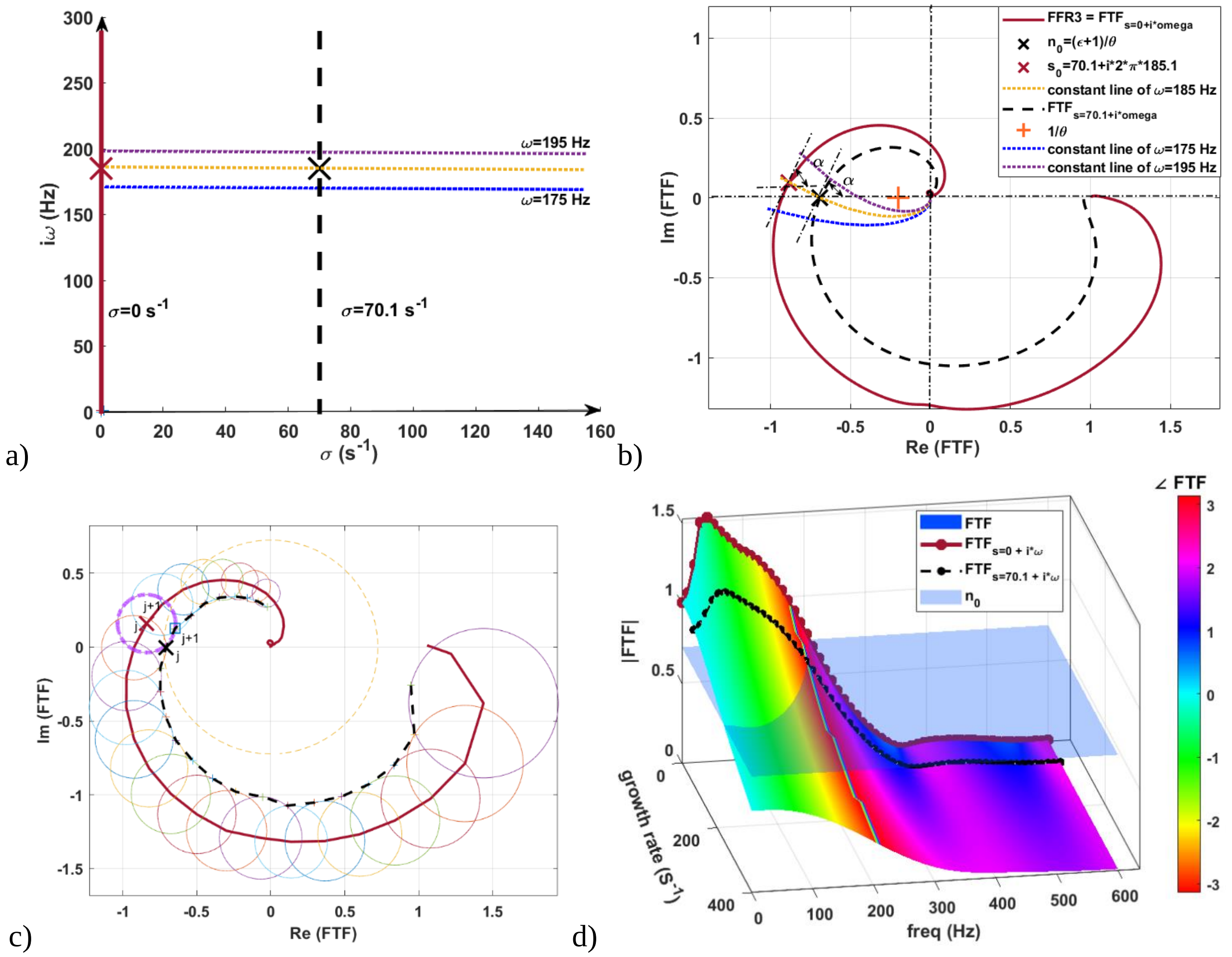

Figure 4: Conformal mapping between (a) s-plane and (b) polar plot of FTF. c) reconstruction one line of the FTF based on the conformality property of causal functions. d) FTF plane.

4. CONCLUSIONS

In this work, an attempt is made to show that the flame frequency response (FFR) is sufficient to study the dilemma of intrinsic thermo-acoustic (in-)stabilities without modeling the flame transfer function (FTF_s) in the complex domain which may generate artificial poles and zeros. It is shown that the causality of the measured flame frequency response can be checked with a straightforward procedure to ensure that there is no unstable pole in the system (RHP pole) and one can use all properties of causal functions. The causality of such systems could help us to find the unstable frequency, growth rate, and even the maximum possible growth rate. A method is proposed how one can reconstruct the FTF_s in the RHP of the complex domain from the FFR by using the conformality property of causal functions and geometrical reconstruction algorithm.

5. ACKNOWLEDGEMENTS

The authors wish to thank the Netherlands Organization for Scientific Research (NWO) for the financial support under project STABLE (16315).

6. REFERENCES

[1] W. Polifke, Black-box system identification for reduced order model construction, Ann. Nucl. Energy. 67 (2014) 109–128. https://doi.org/10.1016/j.anucene.2013.10.037.

[2] T.M. Emmert, State Space Modeling of Thermoacoustic Systems with Application to Intrinsic Feedback, (2016).

[3] A. Cuquel, Dynamics and nonlinear thermo-acoustic stability analysis of premixed conical flames, (2013). http://www.theses.fr/2013ECAP0037/document.

[4] J. Kopitz, W. Polifke, CFD-based application of the Nyquist criterion to thermo-acoustic instabilities, J. Comput. Phys. 227 (2008) 6754–6778. https://doi.org/10.1016/j.jcp.2008.03.022.

[5] B.B.H. Schuermans, W. Polifke, C.O. Paschereit, Modeling transfer matrices of premixed flames and comparison with experimental results, Proc. ASME Turbo Expo. 2 (1999). https://doi.org/10.1115/99-GT-132.

[6] M. Hoeijmakers, Flame-acoustic coupling in combustion instabilities, Technische Universiteit Eindhoven, 2014. https://doi.org/10.6100/IR762773.

[7] T. Emmert, S. Bomberg, W. Polifke, Intrinsic thermoacoustic instability of premixed flames, Combust. Flame. 162 (2015) 75–85. https://doi.org/10.1016/j.combustflame.2014.06.008.

[8] Y. Fourès, I.E. Segal, Causality and analyticity, Trans. Am. Math. Soc. 78 (1955) 385–405. https://doi.org/10.1090/S0002-9947-1955-0069401-5.

[9] J. Bechhoefer, Kramers–Kronig, Bode, and the meaning of zero, Am. J. Phys. 79 (2011) 1053–1059. https://doi.org/10.1119/1.3614039.

[10] L. Knockaert, T. Dhaene, Causality Determination and Time Delay Extraction by Means of the Eigenfunctions of the Hilbert Transform, in: 12th IEEE Work. Signal Propag. Interconnects, IEEE, 2008: pp. 1–4. https://doi.org/10.1109/SPI.2008.4558337 LK - https://tue.on.worldcat.org/oclc/4801497751.

[11] L.L. Barannyk, H.A. Aboutaleb, A. Elshabini, Spectrally Accurate Causality Enforcement using SVD-based Fourier Continuations for High Speed Digital Interconnects, IEEE Trans. Components. 5 (2015) 991–1005. https://doi.org/10.1109/TCPMT.2015.2444388.

[12] J.M. Figueroa-O'farrill, Complex Analysis, in: Math. Tech., 2004: pp. 73–184.

[13] Complex integration, Hong Kong Univ. Sci. Technol. (n.d.). https://www.math.hkust.edu.hk/~maykwok/courses/ma304/06_07/Complex_4.pdf.